Hybrid versus pure-les models comparison for subcritical cylinder flows

Emmanuelle Itam, Stephen Wornom, Bruno Koobus, Alain Dervieux

HYBRID VERSUS PURE-LES MODELS COMPARISON FOR SUBCRITICAL CYLINDER FLOWS

Emmanuelle Itam, Stephen Wornom, Bruno Koobus, Alain Dervieux

1 Introduction

In Computational Fluid Dynamics applications, there is a need for turbulence models which deliver good predictions for flows involving both laminar and turbulent boundary layers, without knowing in advance the regions where turbulence occurs, and then without changing their parameters according to such an *a priori* knowledge of the flow characteristics. In this work, which extends the study [6], we are interested in the assessment of hybrid models for the computation of subcritical flows with laminar boundary layers and in the improvement of the wake behavior prediction in a hybrid RANS/LES model [5, 6, 9]. The performances of a DDES model are compared with a dynamic variational multi-scale (DVMS) large eddy simulation model. The reasons why DDES computations give less good predictions are many. We concentrate in this study on the treatment of the wake. We define RANS/DVMS and DDES/DVMS hybrid models, and compare their predictions with those provided by a DDES model. Three subcritical flows past a circular cylinder are considered, namely at Reynolds numbers 3900, 20000 and 140000 (see Tables 1,2 and 3). Computations are also compared with other LES and hybrid computations in the litterature and with experimental data.

Emmanualle Itam · Bruno Koobus
Institut Montpellirain Alexander Grothendieck(IMAG), Universit de Montpellier, Montpellier, France, e-mail: `{emmanuelle.itam,Bruno.Koobus}@umontpellier.fr`

Stephen Wornom
Socit technologique LEMMA, 2000 route des Lucioles, Sophia-Antipolis, France, e-mail: `stephen.wornom@inria.fr`

Alain Dervieux
Institut National de Recherche en Informatique et en Automatique (INRIA), 2004 Route des lucioles, F-06902 Sophia-Antipolis, e-mail: `alain.dervieux@inria.fr`

2 Numerical model

The spatial discretization is based on a mixed Finite-Element / Finite-Volume formulation on unstructured grids, with degrees of freedom located at vertices i of the tetrahedrization. The finite volume part is integrated on a dual mesh built from medians in 2D and median plans in 3D. The space-discretized unsteady Navier-Stokes equations can be written as follows :

$$\left(\frac{\partial W}{\partial t}, \phi_i\right) + (\nabla \cdot F(W), \phi_i) = -\left(\tau(W), \phi_i\right) \tag{1}$$

where W is the set of conservatives variables and ϕ_i the test function related to vertex i. The diffusive terms $\tau(W)$ are evaluated by a Finite-Element method, whereas a Finite-volume method is used for the convective fluxes $F(W)$. The numerical approximation of the convective fluxes at the interface of neighboring cells is based on the Roe Scheme. In order to obtain second-order accuracy in space, a particular MUSCL-like method is used. The numerical (spatial) dissipation provided by this scheme is made of sixth-order space derivatives and is concentrated on a narrow-band of the highest resolved frequencies. This is expected to limit dissipation of the large scales. This dissipation behaves as O(Δx^5) (on uniform 1D meshes). Lastly, a parameter γ_S directly controls the amount of introduced viscosity and can be explicitly tuned in order to control the influence of numerical dissipation and, when necessary, reduce it to the minimal amount needed to stabilize the simulation. Typically, γ_S is set to a value which gives a 10 times smaller dissipation than the fully-upwind fifth-order scheme. Time integration is performed by a second-order implicit second-order backward difference scheme allowing to address flows at various Mach numbers. In the present paper, the Mach number is chosen equal to 0.1.

3 Turbulence modeling

In the VMS approach [7] which we use, the subgrid-scale (SGS) stress term is acting only on small scales and is computed from the small scale component of the flow field by applying either a Smagorinsky or a WALE SGS model. Further, the constants of these models can be evaluated by a Germano-Lilly dynamic procedure [10]. This results in our *DVMS model*, the semi-discretization of which writes:

$$\left(\frac{\partial \langle W\rangle}{\partial t}, \phi_i\right) + (\nabla \cdot F(\langle W\rangle), \phi_i) = -\left(\tau^{DVMS}(W'), \phi_i'\right). \tag{2}$$

in which the upper index $'$ refers to the resolved small scales. In order to define our hybrid model, we choose a RANS modelling. It is based on the k-ε Goldberg model combined with the Menter correction. We denote it in the sequel as *RANS $k-\varepsilon$-Menter* and write it in short:

$$\Big(\frac{\partial \langle W \rangle}{\partial t}, \phi_i\Big) + (\nabla \cdot F(\langle W \rangle), \phi_i) = -\big(\tau^{RANS}(\langle W \rangle), \phi_i\big). \tag{3}$$

Let us define the hybrid *RANS/DVMS* model based on the above DVMS and RANS models:

$$\Big(\frac{\partial \langle W \rangle}{\partial t}, \phi_i\Big) + (\nabla \cdot F(\langle W \rangle), \phi_i) = -\theta\big(\tau^{RANS}(\langle W \rangle), \phi_i\big) - (1-\theta)\big(\tau^{DVMS}(W'), \phi_i'\big). \tag{4}$$

where W_h denotes the hybrid variables. The symbol $\theta \in [0,1]$ holds for the blending function and is defined as following : $\theta = 1 - f_d(\overline{\theta})$, $\overline{\theta} = tanh(\xi^2)$ with $\xi = \Delta/l_{RANS}$ or $\xi = \mu_{SGS}/\mu_{RANS}$. The shielding function f_d is defined as in DDES, and therefore $f_d \approx 0$ in the boundary layer, and $f_d \approx 1$ outside the boundary layer.

For comparison purpose, we introduce the *DDES* $k-\varepsilon$*-Menter*, written

$$\Big(\frac{\partial \langle W \rangle}{\partial t}, \phi_i\Big) + (\nabla \cdot F(\langle W \rangle), \phi_i) = -\big(\tau^{DDES}(\langle W \rangle), \phi_i\big), \tag{5}$$

in which the above RANS model is introduced in a DDES formulation by replacing in the RHS of the k equations the $D_k^{RANS} = \rho\varepsilon$ dissipation term by $D_k^{DDES} = \rho k^{\frac{3}{2}}/l_{DDES}$ with $l_{DDES} = k^{\frac{3}{2}}/\varepsilon - f_d max\big(0, k^{\frac{3}{2}}/\varepsilon - C_{DDES}\Delta\big)$ where $C_{DDES} = 0.65$ and Δ is a measure of the local mesh size. We have checked in [5] that this model gives predictions close to other DDES approach based on the $k-\omega$ SST model.

Lastly, we define the *DDES/DVMS* model. This version has the same switching as the previous hybrid one, but combines DVMS with the DDES model:

$$\Big(\frac{\partial \langle W \rangle}{\partial t}, \phi_i\Big) + (\nabla \cdot F(\langle W \rangle), \phi_i) = -\theta\big(\tau^{DDES}(\langle W \rangle), \phi_i\big) - (1-\theta)\big(\tau^{DVMS}(W'), \phi_i'\big). \tag{6}$$

Compared to the RANS/DVMS model, and outside the boundary layer where the RANS approach applies, this hybrid model still behaves as DVMS if the grid resolution is sufficient, but it switches to DDES instead of RANS in coarser grid locations. It may also be noted that the LES component (DVMS) of our hybrid models allows a priori a better prediction of the wake than the simpler LES model invoked by DDES.

4 Results

We reconsider here the two first test cases of [6], with several updates and new computations involving other models. A third test case (see Figure 1), which concerns a high subcritical Reynolds number, is also presented for the assessment of the different turbulence models introduced in this work. Among our hybrid models, it turned out that DDES/DVMS performs slightly better, and only its results are reported in the following tables. For reasons of brevity, comments on the results are given with conclusive remarks in the last section.

	$\overline{C}_d$	$-\overline{C}_{p_b}$	C_L^{rms}	L_r	S_t
Experiments					
Norberg [11] min.	0.94	0.83	-	-	-
Norberg [11] max.	1.04	0.93	-	-	-
Parnaudeau [13]	-	-	-	1.51	0.210
Present simulations					
No model	0.87	0.73	0.04	2.11	
RANS $k-\varepsilon$-Menter	0.86	0.72	0.03	2.18	0.216
DDES $k-\varepsilon$-Menter	0.98	0.83	0.10	1.70	0.215
DVMS	1.03	0.86	0.19	1.50	0.216
DDES/DVMS	0.99	0.79	0.12	1.67	0.216
Other simulations					
Kravchenko (LES) [8]	[1.04-1.38]	[0.93-1.23]	-	[1.-1.35]	0.193
D'Alessandro SA-IDDES [1]	0.98	0.83	0.109	1.67	0.214
D'Alessandro $\overline{v}^2-f$ DES [1]	1.02	0.87	0.14	1.42	0.222

Table 1 Bulk quantities for Re=3900 flow around a cylinder. $\overline{C}_d$ holds for the mean drag coefficient, $\overline{C}_{p_b}$ for the mean pressure coefficient at cylinder basis, C_L^{rms} for the root mean square of lift time fluctuations, L_r is the recirculation length, S_t the Strouhal number.

	$\overline{C_d}$	-$\overline{Cp_b}$	C_L^{rms}	Θ_{sep}	L_r	S_t
Experiments						
Norberg [12]	1.16	1.16	0.47	78	1.03	0.194
Present simulations						
No model	1.27	1.35	0.61	82	0.96	
RANS $k-\varepsilon$-Menter	1.31	1.49	0.75	85	0.50	0.212
DDES $k-\varepsilon$-Menter	1.25	1.21	0.58	86	0.90	0.194
DVMS	1.18	1.20	0.46	81	0.96	0.196
DDES/DVMS	1.17	1.13	0.46	82	1.05	0.200
Other simulations						
Salvatici LES [14] min.	0.94	0.83	0.17	-	0.7	-
Salvatici LES [14] max.	1.28	1.38	0.65	-	1.4	-

Table 2 Bulk flow parameters for Re=20000 flow around a cylinder. Θ_{sep} is the separation angle. The other symbols are the same as in Table 1.

	$\overline{C}_d$	$-\overline{C}_{p_b}$	C_L^{rms}	L_r	S_t	Θ_{sep}
Experiments						
Cantwell-Coles [3]	1.24	1.21	-	0.5	0.179	77
Szepessy-Bearman [15]	-	-	0.39	-	-	-
Present simulations						
No model	0.43	0.40	0.14	0.63	0.142	
RANS $k-\varepsilon$-Menter	0.77	0.87	0.31	1.05	0.218	98
DDES $k-\varepsilon$-Menter	0.97	1.01	0.30	0.96	0.217	85
DVMS	1.25	1.33	0.64	0.88	0.217	76
DDES/DVMS	1.04	1.12	0.41	0.91	0.214	85
Other simulations						
Froehlich (LES Smago.) [4]	1.16	1.33	-	0.41	0.217	94
Breuer (LES Smago. Dyn) [2]	1.24	1.40	-	0.57	0.204	96

Table 3 Bulk quantities for Re=140000 flow around a cylinder. Same symbols as in Table 2.

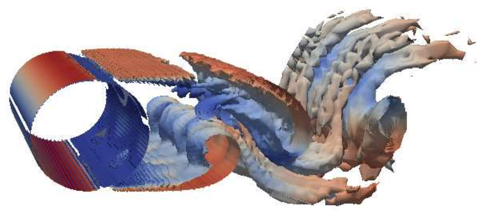

Fig. 1 Iso-contours of Q-criterion colored by velocity magnitude obtained with RANS/DVMS model for Re=140000 flow around a cylinder.

5 Comments and conclusions

In the lines of [6], DVMS, DDES and our hybrid model are compared for subcritical flows past cylinders.

For low and medium subcritical Reynolds numbers (Re = 3900 and Re = 20000), the computations performed with the turbulent models mentioned above compare well with experimental data and numerical results in the litterature. Several remarks can however be made. First, although theoretically not adapted (the laminar boundary layer is computed by a RANS model), the DDES and our hybrid approach provide a reasonably good prediction of main outputs. As noticed in [1], the eddy viscosity introduced in the attached boundary layer is small enough so that its effect is negligible. Second, the DDES and our hybrid model predictions are generally less accurate than those obtained with DVMS for Reynolds number 3900, which is a LES model of intermediate sophistication. Third, comparing our hybrid approach and DDES, we observe that an overall improvement is obtained for Reynolds number 20000 when a better LES component is locally imposed (through the use of DVMS in the wake region).

For a higher subcritical Reynolds number (Re = 140000), while DVMS behaves correctly, the RANS, DDES and our hybrid turbulence models predict a turbulent boundary layer and are then not accurate. The DDES/DVMS model shows intermediate prediction with a reasonable improvement with respect to DDES. However, still only LES-type simulations provide bulk quantities prediction inside a 10% interval. DDES results and our hybrid model predictions are in a 20% interval, with a slight improvement for our hybrid approach. These models still need further improvements for properly tackling such subcritical flows.

Acknowledgements This work has been supported by French National Research Agency (ANR) through project MAIDESC n^o ANR-13-MONU-0010. This work was granted access to the HPC resources of CINES under the allocations 2017-A0022A05067 and 2017-A0022A06386 made by GENCI (Grand Equipement National de Calcul Intensif).

References

1. V. DAlessandro, S. Montelpare, and R. Ricci. Detached eddy simulations of the flow over a cylinder at Re = 3900 using Open- FOAM a low-diffusion MUSCL scheme for LES on unstructured grids. Computers and Fluids, 136:152169, 2016.
2. M. Breuer. A challenging test case for large eddy simulation, high Reynolds number circular cylinder flow. International Journal of Heat and Fluid Flow, 21, 648-654, 2000.
3. B. Cantwell and D. Coles. An experimental study of entrainment and transport in the turbulent near wake of a circular cylinder. Journal of Fluid Mechanics, 136, 321-374, 1983.
4. J. Froehlich, W. Rodi, J.P. Bertoglio, U. Bieder and H. Touil. Large Eddy Simulation of Flow around Circular Cylinders on Structured and Unstructured Grids I. Ed.: E.H. Hirschel. Numerical flow simulation II. 75, 231-249, Vieweg, 2001.
5. E. Itam, S. Wornom, B. Koobus and A. Dervieux. Application of a Hybrid Variational Multiscale Model to Massively Separated Flows. 3AF, Toulouse, France, March 2015.
6. E. Itam, S. Wornom, B. Koobus, and A. Dervieux. Hybrid simulation of high-Reynolds number flows relying on a variational multiscale model. 6th Symposium on Hybrid RANS-LES Methods, Strasbourg, France, 26-28 September 2016.
7. B. Koobus and C. Farhat. A variational multiscale method for the large eddy simulation of compressible turbulent flows on unstructured meshes-application to vortex shedding. Comput. Methods Appl. Mech. Eng. 193, 13671383, 2004.
8. A.-G. Kravchenko and P. Moin. Numerical studies of flow over a circular cylinder at Re_D=3900, Phys. Fluids, 12:2, 403-417, 2000.
9. C. Moussaed, M.V. Salvetti, S. Wornom, B. Koobus, and A. Dervieux. Simulation of the flow past a circular cylinder in the supercritical regime by blending RANS and variational-multiscale LES models. Journal of Fluids and Structures, 47:114123, 2014.
10. C. Moussaed, S. Wornom, M.V. Salvetti, B. Koobus and A. Dervieux. Impact of dynamic subgrid-scale modeling in variational multiscale large-eddy simulation of bluff body flows. Acta Mechanica, 12:33093323, 2014.
11. C. Norberg. Effects of Reynolds number and low-intensity freestream turbulence on the flow around a circular cylinder. Publ. No.87/2, Department of Applied Thermosc. and Fluid Mech., Chalmer University of Technology, Sweden, 1987.
12. C. Norberg. Fluctuating lift on a circular cylinder: review and new measurements. J. Fluids Struct., 17:5796, 2003.
13. P. Parnaudeau, J. Carlier, D. Heitz, and E. Lamballais. Experimental and numerical studies of the flow over a circular cylinder at Reynolds number 3900. Phys. Fluids, 20(085101), 2008.
14. E. Salvatici and M.V. Salvetti. Large eddy simulations of the flow around a circular cylinder: effects of grid resolution and subgrid scale modeling, Wind and Structures, 6:6, 419-436, 2003.
15. S. Szepessy and P. W. Bearman. Aspect ratio and end plate effects on vortex shedding from a circular cylinder. J. Fluid Mech. 234, 191217, 1992.